Compressive Strength of Reinforced Concrete Disks with Transverse Tension

Hoang, Linh Cao; Jacobsen, Hans J.; Larsen, Bo

Published in:
Bygningsstatiske Meddelelser

Publication date:
2012

Document Version
Publisher's PDF, also known as Version of record

Årgang LXXXIII, Nr. 2-3, juli 2012

BYGNINGSSTATISKE MEDDELELSER

udgivet af

DANSK SELSKAB FOR BYGNINGSSTATIK

Proceedings of the Danish Society for Structural Science and Engineering

KØBENHAVN 2012

ISSN 0106-3715 (trykt udgave)
ISSN 1601-6548 (online)

Årgang LXXXIII, Nr. 2-3. juli 2012

BYGNINGSSTATISKE MEDDELELSER

udgivet af

DANSK SELSKAB FOR BYGNINGSSTATIK

Proceedings of the Danish Society for Structural Science and Engineering

KØBENHAVN 2012

Artikler offentliggjort i Bygningsstatiske Meddelelser har gennemgået review.

Papers published in the Proceedings of the Danish Society for Structural Science and Engineering have been reviewed.

Compressive Strength of Reinforced Concrete Disks with Transverse Tension

BYGNINGSSTATISKE MEDDELELSER
Proceedings of the Danish Society for Structural Science and Engineering
Edited and published by the Danish Society for Structural Science and Engineering
Volume 83, No. 2-3, 2012, pp.23-61

Compressive Strength of Reinforced Concrete Disks with Transverse Tension

Linh C. Hoang [1]
Hans J. Jacobsen [2]
Bo Larsen [2]

1. Introduction

It is well-known that the compressive strength of reinforced concrete disks is reduced when the compressive stress field is crossed by tensioned reinforcing bars. Numerous tests have demonstrated this tendency and it is commonly accepted that the strength reduction is mainly a result of different forms of cracks induced by the transverse tension. The subject represents a basic problem in concrete mechanics and has great relevance in practice. This is so because reinforced concrete structures are often subjected to plane stress states that involve a uniaxial com-

[1] Professor, Ph.D., Faculty of Engineering, University of Southern Denmark
[2] M.Sc., Faculty of Engineering, University of Southern Denmark

pression field in the concrete and tensile stresses in an orthogonal reinforcement mesh.

When structural concrete members are designed by use of plasticity methods, it is necessary to operate with a reduced compressive strength of concrete. This strength parameter, referred to as *the effective strength*, is obtained by multiplying the reference cylinder strength with a so-called *effectiveness factor*, ν. At present, different formulas for ν must be adopted for different stress conditions. These formulas are usually found empirically by calibrating the theoretical plastic solutions with test results. From a practical point of view, however, it is desirable to have a more general ν-formula that is valid for a variety of plane stress states. Such a formula must, at least, be able to deal with the strength reduction of compression fields crossed by reinforcement stressed to tension - a condition often met in practice. This is the main reason for the study presented in this paper.

Several formulas for the strength reduction have been proposed. This include the works by Vecchio & Collins (1982), Kollegger (1988), Roos (1994), Belarbi & Hsu (1995), Zhang (1997) and Fehling *et al.* (2008) - just to mention a few. When reviewing the previous works, two interesting observations stand out. First, almost all proposed formulas express the strength reduction as a function of the transverse tensile strain. Second, there seems to be a lack of consensus regarding a maximum strength reduction. Vecchio & Collins (1982) as well as Belarbi & Hsu (1995) proposed their formulas on the basis of own tests. They found, for very large tensile strains, strength reductions down to about 20 – 30 % of the cylinder strength. In the formula by Roos (1994), which is based on a critical selection of published tests, a reduction to app. 40 % of the cylinder strength is obtained for transverse strains up to 3.5 %. Fehling *et al.* (2008), on the other hand, proposed a lower limit of about 50 % strength reduction when the transverse strain exceeds approximately 0.8 %. Quite differently, Kollegger (1988) worked with a lower limit of 80 % of the cylinder strength.

The lack of consensus regarding a maximum strength reduction may probably be explained by the fact, that the various authors have used different selection of tests, but all formulated their formulas on the basis of the transverse strain without account of the reinforcement ratio. A formula of this type will predict the same strength reduction for disks subjected to the same magnitude of transverse strain, regardless of the reinforcement content. This is unlikely in reality since the reinforcement ratio has a great influence on the crack distance (i.e. the distance between adjacent primary cracks) as well as the extent of internal, secondary cracking.

In view of the above, we will in the following develop a ν-formula which depends both on the reinforcement stress as well as the reinforcement ratio. The formula is a further development of the ideas introduced by Zhang (1997). Comparison with 127 test results shows satisfactory agreement.

Although the formula (unlike the purely strain based formulas) is able to differentiate between disks with identical transverse strain but different reinforcement ratios, there is a limitation. As will be discussed, the underlying assumptions will restrict us from using the formula in situations where the transverse strain is several times the reinforcement yield strain. According to tests, a significant increase of strain beyond the yield strain will cause further strength reduction, even though the transverse tension remain practically unchanged (corresponding to the yield stress of the reinforcement). Inclusion of this effect requires further work. Ideas for further development will be discussed.

2. Formula for Strength Reduction

2.1 Problem statement

Figure 2.1 shows a concrete disk reinforced with deformed bars in the transverse direction. The disk is loaded with a uniform compressive stress, σ_c, in the vertical direction and a uniform tensile stress, σ_t, in the transverse direction. The problem we wish to study in the following is how to determine the maximum compression stress when $\sigma_t > 0$. In the case with $\sigma_t = 0$, we have a uniaxial stress condition with $\sigma_c = f_{cs}$, where f_{cs} denotes the uniaxial compressive strength of the disk. It is important already now to clarify, that the uniaxial compressive strength of a concrete disk – as found from tests – is usually different from the standard cylinder strength f_c. Therefore, when evaluating the strength reduction due to transverse tension in a disk, we have to use f_{cs}, and not f_c, as the reference strength.

Figure 2.1 Reinforced concrete disk loaded in biaxial tension-compression.

2.2 Basic assumptions

We know from tests that the compressive strength of a disk is reduced, i.e. $\sigma_c < f_{cs}$, when the transverse tension begins to induce cracks. In the following, we distinguish between two systems of cracks. First, there are the primary cracks (also called macro cracks) formed parallel to the compression direction, see Figure 2.2. The average distance between adjacent primary cracks is called a. Second, there

are the inclined internal cracks (also referred to as micro- or secondary cracks). The internal cracks are formed near the intersections between the primary cracks and the reinforcement bars. According to Zhang (1997) the strength reduction may be attributed to the development and the extent of internal cracks. This crucial role of internal cracking will also be our starting point. Note, however, that the below description of the cracking process is very schematic and only serves as a way to establish (qualitatively) a suitable formula to calculate the strength reduction. Details of the real cracking process in members loaded in tension have been described by e.g. Goto (1971) and Goto and Otsuka (1979).

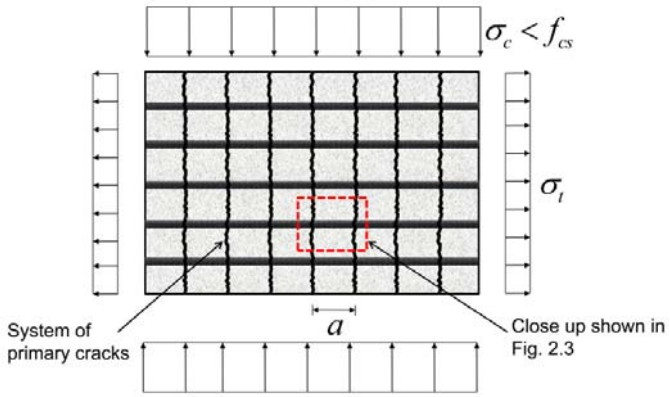

Figure 2.2 Reinforced disk with system of primary cracks.

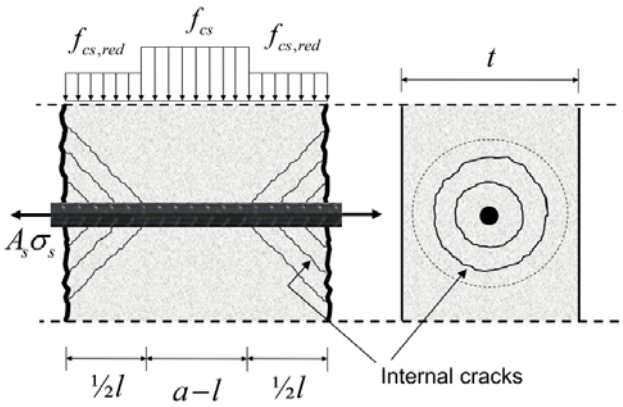

Figure 2.3 Reduced strength in zones with internal cracks.

Figure 2.3 shows two adjacent primary cracks at the distance a. The cracks are crossed by a reinforcement bar that transfers a tensile force $T = A_s\sigma_s$. For simplicity, we assume the disk to be reinforced only with one layer of reinforcement placed in the middle plane of the disk. After the development of the primary cracks and as a consequence of an increase in the reinforcement stress, σ_s, a system of three dimensional internal cracks is developed. These internal cracks may

be envisaged as a kind of local punching failures caused by the bursting stresses from the ribbed bars. For simplicity, we assume the punching failure surfaces to be cone shaped. The extent of internal cracking and thus the size of the concrete cones depend on the tensile force in the reinforcement. We characterize the extent of internal cracking with a so-called *penetration length l*, see illustration in Figure 2.3.

The internal cracks introduce local damages in the concrete. It is therefore reasonable to assume that the compression stress transmitted through zones with internal cracks must be reduced in comparison with the strength of uncracked concrete. The simplest way to reflect this is to consider a stress distribution at the ultimate state as depicted in Fig. 2.3. In the undamaged zone with length ($a - l$), the full compressive strength f_{sc} may be transferred. Within the zones with internal cracking, however, we assume an average, reduced strength $f_{cs,red}$. Now, the system of internal cracks is three dimensional. It is therefore reasonable to expect that the extent of local damages across the thickness of the disk will increase as the penetration length l increases. This has been illustrated in Figure 2.3 (to the right) where different punching cone diameters have been indicated. It follows from the above argument that $f_{cs,red}$ cannot be taken as a constant value. Remember that $f_{cs,red}$ reflects the average strength reduction within l and across the thickness. Hence, we must work with a model where $f_{cs,red}$ decreases as the penetration length l increases. This has been illustrated in Figure 2.4.

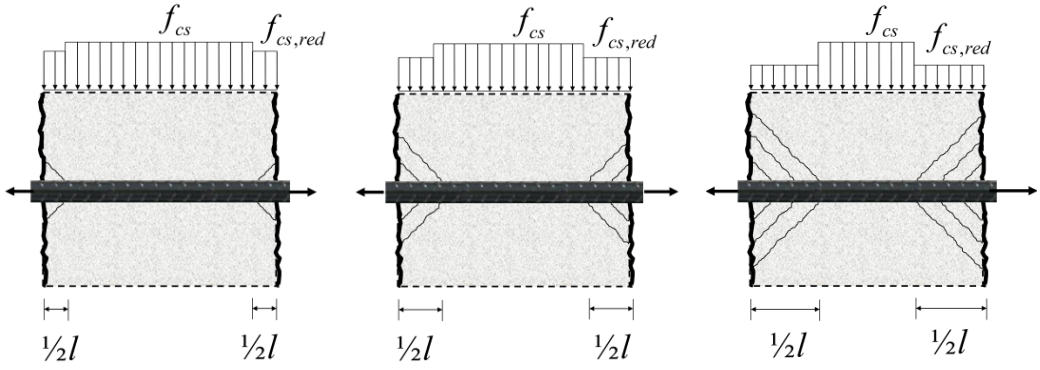

Figure 2.4 Evolution of $f_{cs,red}$ and penetration length l for increasing reinforcement stresses.

In the following, we assume a simple linear decrease of $f_{cs,red}$ with respect to the penetration length l, i.e.:

$$f_{cs,red} = \left(1 - \eta \frac{l}{a}\right) f_{cs} \tag{2.1}$$

where η is less than unity and may be called *the damage factor*. This factor will be determined by calibration with test results.

According to the stress distribution shown in Figures 2.3 and 2.4, we will have maximum reduction of strength when $f_{cs,red}$ is transferred across the whole crack

distance a. This corresponds to a situation where internal cracking has entirely penetrated the zones between adjacent macro cracks. Thus, when inserting $l/a = 1$ into (2.1), we find $f_{cs,red} = (1-\eta)f_{cs}$, which we may interpret as the compressive strength of the internally "fully cracked" concrete. The interesting question here is whether we can assume a constant value for η and thereby obtain a lower limit for the strength of internally cracked concrete? This is not likely.

It would be more reasonable to expect that once fully cracked, further reduction of concrete strength may take place if the crack widths increase. This implies that the damage factor η should depend on the crack width. However, with the present state of knowledge it is premature to speculate further in this direction. For the time being, we are only able to determine η by calibration with test results. Further, we will have to limit the postulated effects on the variation of η by limiting the range of crack widths. This will be done by only considering tests, where the transverse strain is smaller than or in the order the reinforcement yield strain ε_y. By imposing this limitation, we also maintain a unique relationship between the reinforcement strain ε_s and the reinforcement stress σ_s, which as shown later will be a parameter in the ν-formula.

Now, to determine the load carrying capacity of the disk, we need to find the resultant of the stress distribution shown in Figure 2.3. The stress resultant is thereafter used to calculate an average compressive stress, σ_c, which is then interpreted as the reduced compressive strength of the disk due to transverse tension. The following condition applies:

$$\sigma_c a t = f_{cs} t(a-l) + 2 \cdot \frac{l}{2} t f_{cs} \left(1 - \eta \frac{l}{a}\right) \tag{2.2}$$

which leads to:

$$\sigma_c = f_{cs} \left(1 - \eta \left(\frac{l}{a}\right)^2\right) \tag{2.3}$$

With formula (2.3) we have now reached the first step of our objective, namely to find a suitable structure for a ν-formula:

$$\nu = \frac{\sigma_c}{f_c} = \frac{f_{cs}}{f_c} \left(1 - \eta \left(\frac{l}{a}\right)^2\right) \tag{2.4}$$

In (2.4) we have introduced f_c in order to keep the original definition of ν as a strength reduction factor measured relative to the standard uniaxial compressive strength obtained from laboratory tests with 150mm x 300mm concrete cylinders.

The next steps will be to quantify the crack distance a, and to estimate the internal crack penetration length l as a function of the applied transverse tensile stress.

2.3 The macro crack distance

A model to describe the crack widths and the crack distance a of a fully developed macro crack system can found in Nielsen (2005). According to this model, the crack distance may be estimated as follows:

$$a = \frac{d}{8\rho} \tag{2.5}$$

Here d is the reinforcement diameter and ρ is the reinforcement ratio. The formula applies to deformed bars. For plain bars, a factor 2 is introduced on the right hand side of the formula. In this paper, only deformed bars will be considered.

2.4 Penetration length of internal cracking

To make formula (2.4) useful in practice, we need to establish a relationship between the penetration length of internal cracking, l, and the reinforcement tensile force. The aim is not to establish a complete formula. Rather, we seek only to establish a qualitatively and simple relationship.

We consider again a reinforcement bar stressed to σ_s, see Figure 2.3. The development of a cone shaped internal crack surface can, as mentioned, be envisaged as the development of a local punching failure surface around the reinforcement bar. From analyses of punching in slabs, see e.g. Nielsen & Hoang (2011), we know that the punching load depends on the area as well as the geometry of the failure surface (i.e. the yield line). To simplify, we assume here that the punching load, at least approximately, is proportional to the area of the failure surface. Furthermore, the punching load is, according to test results, approximately proportional to the tensile strength of concrete, f_t. In the present problem, the reinforcement force, $T = A_s\sigma_s$, is the punching load. This means that we can assume the following relation:

$$A_s\sigma_s \propto A_{surface} f_t \tag{2.6}$$

$A_{surface}$ denotes the area of a conical crack surface and may be determined as follows:

$$A_{surface} = \pi r\sqrt{h^2 + r^2} \tag{2.7}$$

where r is the cone radius and h is the cone height, which here may be taken as $0.5l$. Now, without loss of generality, we may take r as a fraction of h and rewrite $A_{surface}$ as follows:

$$A_{surface} = kl^2 \tag{2.8}$$

with k being a constant.

By inserting (2.8) into (2.6) we find:

$$A_s\sigma_s \propto l^2 f_t \tag{2.9}$$

From (2.9) we are now able to deduce that the penetration length l must be proportional to $\sqrt{(\sigma_s / f_t)}d$ because $A_s = \frac{\pi}{4}d^2$. Hence, the following important relation can be established

$$l = C\sqrt{\frac{\sigma_s}{f_t}}d \tag{2.10}$$

where C for the time being is an unknown factor. This factor must be determined by calibration with test results. Note that a geometrical restriction, $l \le a$, must be imposed on formula (2.10). In the limiting case with $l = a$, we will have internal cracks over the entire zone between adjacent macro cracks.

2.5 The effectiveness factor

We have now identified a number of mechanical and geometrical parameters that influence the strength reduction. Further, we have established a formula for the strength reduction. What is left to do is to quantify η and C through calibration with test results. This will be done in the next Chapter.

For convenience, we first rewrite formula (2.4) by replacing a and l with the right hand sides of formulae (2.5) and (2.10). This leads to:

$$\nu = \frac{\sigma_c}{f_c} = \begin{cases} \dfrac{f_{cs}}{f_c}\left(1-\eta\chi^2\right), \text{ for } \chi \le 1 \\ \\ \dfrac{f_{cs}}{f_c}\left(1-\eta\right), \quad \text{for } \chi \ge 1 \end{cases} \tag{2.11}$$

where

$$\chi = 8C\sqrt{\frac{\sigma_s}{f_t}}\rho \tag{2.12}$$

The tensile strength of concrete, f_t, will in this paper be calculated by using the Danish formula:

$$f_t = \sqrt{0.1 f_c} \tag{2.13}$$

Note that in formula (2.11) we have incorporated the above mentioned geometrical restriction $l \le a$. This means that l/a must be taken as unity when the right hand side of (2.10) leads to values larger than a. We have in (2.11) deliberately replaced l/a with the symbol χ to make sure that this quantity is not given a physical meaning for values larger than unity. The schematic variation of formula (2.11) has been shown in Figure 2.5.

As stated above, the present work rests on some ideas introduced by Zhang (1997), who also operated with a kind of penetration length of internal cracking. However, the expression by Zhang differs from Equation (2.10). This eventually means that the parameter that should be equivalent to χ appears with $\sqrt{\rho}$ instead of ρ.

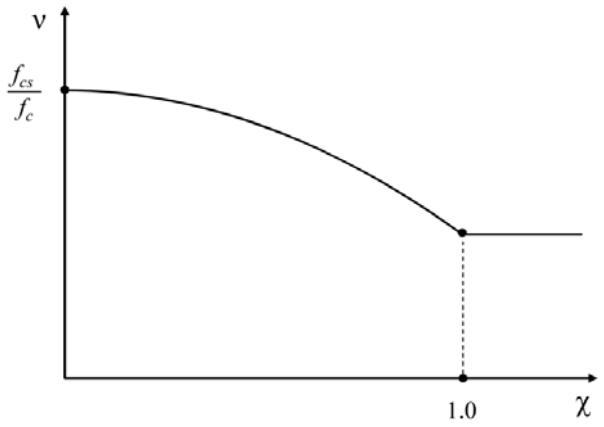

Figure 2.5 Schematic variation of the effectiveness factor as a function of χ.

2.6 Strength reduction in diagonal compression fields

Formula (2.11) was developed for the loading condition shown in Figure 2.1 and is therefore strictly speaking only valid for this case. However, in practice the concrete stress field can form any angle with the reinforcement directions.

One way to cover the different stress states is to develop formulas along the same line as above. In the following we will not make any attempt in this direction. However, it seems reasonable to expect that the structure of such formulas will resemble what we have in (2.11). Of course, estimates of the crack distance and the penetration length may be more complicated when the compression field is not perpendicular to the tensile reinforcement. In any case, what this eventually means is that η and C might be different for different loading configurations.

For use in practice, we may therefore settle with formula (2.11) and adopt different sets of η and C to cover different loading cases. Fortunately, as will be shown in Chapter 3, η and C are not too sensitive with regards to the loading configuration. It will be shown that one single set of η and C is sufficient to cover all the different loading configurations used in tests.

3. Calibration of ν-formula with test results

The proposed ν-formula (2.11) contains two dimensionless parameters η and C, which may be determined by calibration with test results. For this purpose, a large number of test results from the literature have been collected.

3.1 Collected test results

A critical review of the collected test results has been carried out. The purpose was to select tests suitable for comparison with the ν-formula. One of the criteria in this context was to consider only tests with transverse strains less than or in the order of the reinforcement yield strain, ε_y (see also discussion in Section 2.2). For reinforcement types without a well-defined yield plateau, the strain corresponding to $f_{0.2\%}$ is normally used as a nominal yield strain. For pure shear tests, only cases with $\sigma_s < f_y$ have been considered (see discussion in Section 3.2.3).

The test results were extracted either from the original references (Schlaich & Schäfer, 1983; Kollegger & Mehlhorn, 1988; Kollegger, 1988; Schieβl, 2005; Dyngeland, 1989; Demorieux, 1969; Yamaguchi & Naganuma, 1991; Pang & Hsu, 1995; Taniguchi 1990) or from the review reports by Fehling *et al.* (2008) and Roos (1994).

A total number of 127 test results have been selected. An overview of the selected tests may be found in the Appendix. For details, the reader is referred to Jacobsen & Larsen (2010), the background document to this paper.

3.2 Experimental loading conditions

The variety of test setups reported in the literature can basically be condensed down to three loading conditions as illustrated in Figure 3.1. The three basic cases are described below. It is important to note that the way the maximum concrete stress, σ_c, is determined from the experimental measurements will depend on the loading condition.

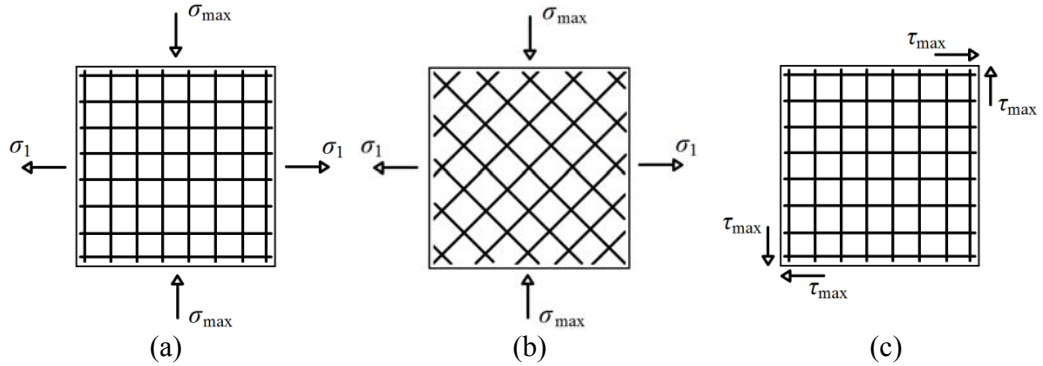

Figure 3.1 Tension-compression with reinforcement layout θ = 0˚/90˚ (a) and θ = ±45˚ (b); pure shear (c).

3.2.1 Tension-compression, $\theta = 0^\circ/90^\circ$

The loading condition tension-compression with $\theta = 0^\circ/90^\circ$ is illustrated in Figure 3.1(a). This test setup is the best representation of the conditions assumed for the proposed ν-formula. Many of the specimens tested with this setup were provided with an orthogonal reinforcement mesh forming the angles $\theta = 0^\circ$ and $\theta = 90^\circ$ with the compression direction. As input to the ν-formula, the transverse reinforcement stress σ_s is determined as

$$\sigma_s = \frac{\sigma_1}{\rho_1} \tag{3.1}$$

where σ_1 is the applied tensile stress and ρ_1 is the transverse reinforcement ratio. Since the specimens also have reinforcement parallel to the compression direction, it is necessary to deduct the compressive reinforcement stresses from the experimental results in order to find the maximum compressive concrete stress, σ_c. The following formula (also used by Roos (1994)) has been used:

$$\sigma_c = \sigma_{\max} - \sigma_{s,2}(\varepsilon_2)\rho_2 \tag{3.2}$$

where $\sigma_{\max}$ is the maximum compression stress applied to the test specimen (applied force divided by the concrete cross-sectional area A_c), ρ_2 is the reinforcement ratio in the compression direction and $\sigma_{s,2}(\varepsilon_2)$ is the stress in the compression reinforcement. This stress is determined as a function of the compressive strain ε_2 measured at the time when $\sigma_{\max}$ is applied.

3.2.2 Tension-compression, θ = ±45°

Figure 3.1(b) shows the loading condition tension-compression, $\theta = \pm 45^\circ$. The orthogonal reinforcement forms the angles $\theta = \pm 45^\circ$ with the principal directions. In case of isotropic reinforced specimens, i.e. same reinforcement ratio ρ in both directions, we may calculate the tensile reinforcement stress σ_s by using formula (3.1). The maximum compressive concrete stress σ_c is determined as follows when the reinforcement is well-anchored at the faces subjected to compression:

$$\sigma_c = \sigma_1 + \sigma_{\max} \tag{3.3}$$

Here, $\sigma_{\max}$ is the maximum recorded external applied compression stress.

3.2.3 Pure Shear

Pure shear tests require more sophisticated equipment to carry out than the tension-compression tests. This is why some investigators choose to conduct tension-compression tests with $\theta = \pm 45^\circ$ instead. This will give pure shear (see Figure 3.1(c)) in the reinforcement directions when the applied compression $\sigma_{\max}$ equals the applied tension σ_1. Some investigators, however, have carried out direct pure shear tests. In isotropic reinforced specimens subjected to pure shear, the com-

pressive concrete stress σ_c forms an angle $\theta = 45^\circ$ with the reinforcement directions. The reinforcement stress σ_s may therefore be found as follows:

$$\sigma_s = \frac{\tau_{max}}{\rho} \tag{3.4}$$

Here, τ_{max} is the tested ultimate shear strength and ρ, as before, is the reinforcement ratio. The maximum concrete stress σ_c is given by:

$$\sigma_c = 2\tau_{max} \tag{3.5}$$

Note that in a pure shear test setup, σ_s and σ_c are related to each other through equilibrium requirements. This means that only over-reinforced specimens (i.e. $\sigma_s < f_y$) should be considered when results of pure shear tests are used to determine the reduced compressive strength. Therefore, over-reinforced isotropic specimens have been considered in this paper in the case of pure shear.

3.3 Results

The test results collected in the Appendix have been used to determine the parameters η and C in the proposed ν-formula. The tested strength reductions, σ_c/f_c, tabulated in the Appendix will in the following also be termed ν_{test}.

To carry out the calibration of the ν-formula with test results, we need first to determine f_{cs}/f_c; the ratio between the uniaxial compressive strength of the disk and the reference cylinder strength. This is done by considering specimens tested in uniaxial compression. Within each test series, or sub-series, where the uniaxially loaded specimens are similar, we determine f_{cs}/f_c as the average of test results. The results are summarized in Table 3.1.

It is seen from Table 3.1 that the ratio f_{cs}/f_c differs from series to series. This may partly be explained by the differences in specimen geometry and in strength development of specimens and of cylinders. Other factors such as the casting direction, compacting methods, boundary conditions in the test setup, etc., may have an impact as well. What we see is that f_{cs} is generally smaller than f_c. Exceptions are observed for the tests by Schieβl (2005) and by Kollegger (1988). It must be emphasized that the statistic basis for f_{cs}/f_c is different for each of the individual test series. This is so because the number of available uniaxial tests is different from series to series. In total, we have 32 uniaxial compression tests available to determine f_{cs}/f_c. For the tests by Taniguchi (1990) and by Pang & Hsu (1995), we do not have any uniaxial tests at all. In this case, we have assumed $f_{cs}/f_c = 0.90$ corresponding to the average value obtained from the other series.

Having determined f_{cs}/f_c for each series, it is now possible to seek for the set of η and C that overall gives the best agreement with test results. It turns out that by adopting $\eta = 0.50$ and $C = 0.244$, we obtain the best agreement.

Table 3.1 Results of calibration with $C = 0.244$ and $\eta = 0.50$.

Test series	Loading type	$\frac{f_{cs}}{f_c}$	$\frac{\nu_{test}}{\nu_{cal}}$		Group number (series with comparable f_{cs}/f_c)
			Mean value	Standard deviation	
Schlaich & Schäfer (1983)	*u, b*	0.95	1.00	0.12	1
Demorieux (1969)	*u, b*	0.87	1.08	0.23	2
Schieβl (2005)	*u, b*	1.09	0.92	0.08	3
Eibl & Neuroth (1988)	*u, b*	0.80	0.99	0.07	4
Kollegger & Mehlhorn (1988)	*u, b*	0.93	0.97	0.07	1
Fehling et al. (2008)	*u, b*	0.75	0.97	0.14	5
Dyngeland (1989)	*u, b*	0.94	1.02	0.06	1
Kollegger (1988)	*u, b*	1.03	0.97	0.05	6
Yamaguchi & Naganuma (1991)	*u, b, s*	0.88	1.18	0.20	2
Taniguchi (1990)	*b*	-	0.90	0.07	7
Pang & Hsu (1995)	*b*	-	0.78	0.11	7
Average for all 127 tests	-	0.90	1.00	0.145	

Notations: *u*: uniaxial compression
b: biaxial tension-compression
s: pure shear

The calibration results are summarized in Table 3.1. The mean value of the ratio between tested and calculated strength, i.e. $\sigma_{c,test}/\sigma_{c,cal} = \nu_{test}/\nu_{cal}$, are shown for each series as well as for all 127 tests. The overall result is $\nu_{test}/\nu_{cal} = 1.0$ with a standard deviation of 0.145. Note that with the exception of the tests by Demorieux (1969) and by Yamaguchi & Naganuma (1991), we find within each test series a standard deviation smaller than 0.145.

The results appear in Figure 3.2. Here, we see that some of the results (both tested and calculated) are larger than 1.0. This is so because we define the strength reduction relative to f_c, which for some series is smaller than f_{cs}.

To further study the tendency of the test results, we now assemble the test series into seven groups. Each group contains test series with comparable values of f_{cs}/f_c. The group numbering may be found in Table 3.1. As an example, we have in Group 1 assembled test series with f_{cs}/f_c between 0.93 - 0.95.

The results for each group have been compared with the ν-formula in Figures 3.3 - 3.9. In each figure, we have taken f_{cs}/f_c as the average value within each group. It can be seen that the agreement for Groups 1, 4 and 6 is quite reasonable while it is less impressive for the remaining groups.

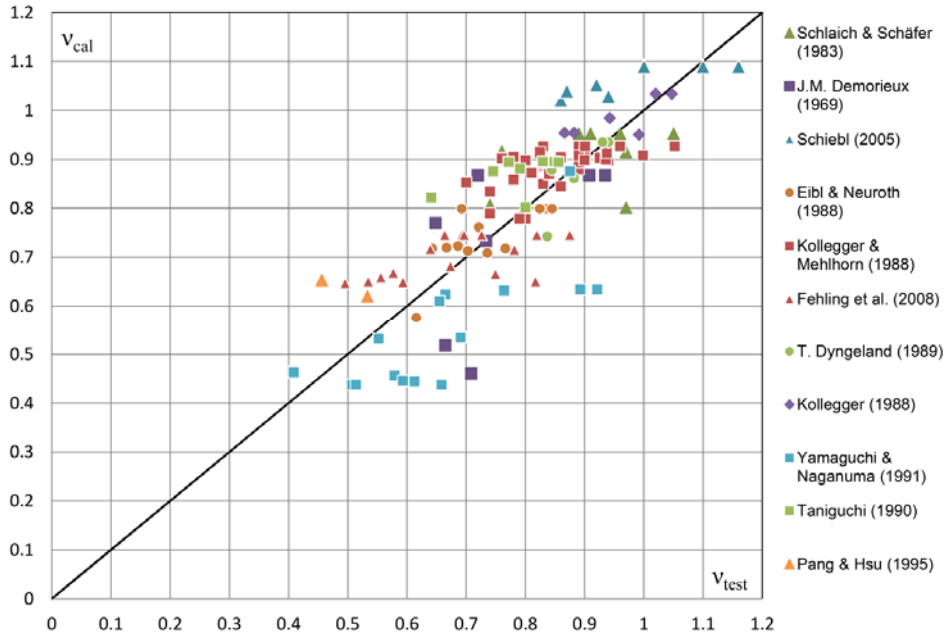

Figure 3.2 Calculated strength reduction vs. tested strength reduction for all 127 tests. Mean value ν_{test}/ν_{cal} = 1.0 and standard deviation = 0.145.

It must be emphasized here that the results have been obtained by fixing the model parameters to C = 0.244 and η = 0.5. However, as discussed in Section 2.6, it might be reasonable to adopt different sets of η and C depending on the loading conditions and the angle at which the compression field crosses the tensile reinforcement. If doing so, we might be able to reduce the rather large scatter found for Group 2 in Figure 3.4. This group contains both tension-compression tests (with $\theta = 90^o$ as well as $\theta = \pm 45^o$) and pure shear tests. Calibration of the formula by adopting different values of η and C will not be examined further in this paper for the simple reason that the result already obtained is satisfactory (at least for practical use).

Other aspects, such as the number of reinforcement layers, the reinforcement spacing and the concrete cover, might also influence the parameters C and η. Some of these aspects have been considered by Jacobsen & Larsen (2010) in order to refine the formula. Slightly better results were obtained.

The results presented above are based on the fact that each test series has different value of f_{cs}/f_c. It might be interesting to investigate the scenario, where we just adopt one single value; namely f_{cs}/f_c = 0.90 corresponding to the mean value of all 32 uniaxial tests. It turns out that in this case, we find C = 0.248 (which is quite

close to the result above) when we fix $\eta = 0.5$. The standard deviation in this case of course becomes larger, namely 0.165.

The obtained results should be viewed in relation to the results found by using the ν-formula proposed by Zhang (1997). This formula renders a mean value of 0.97, which is quite satisfactory. The standard deviation, however, amounts to 0.28 which is less impressive. The calculations may be found in Jacobsen & Larsen (2010).

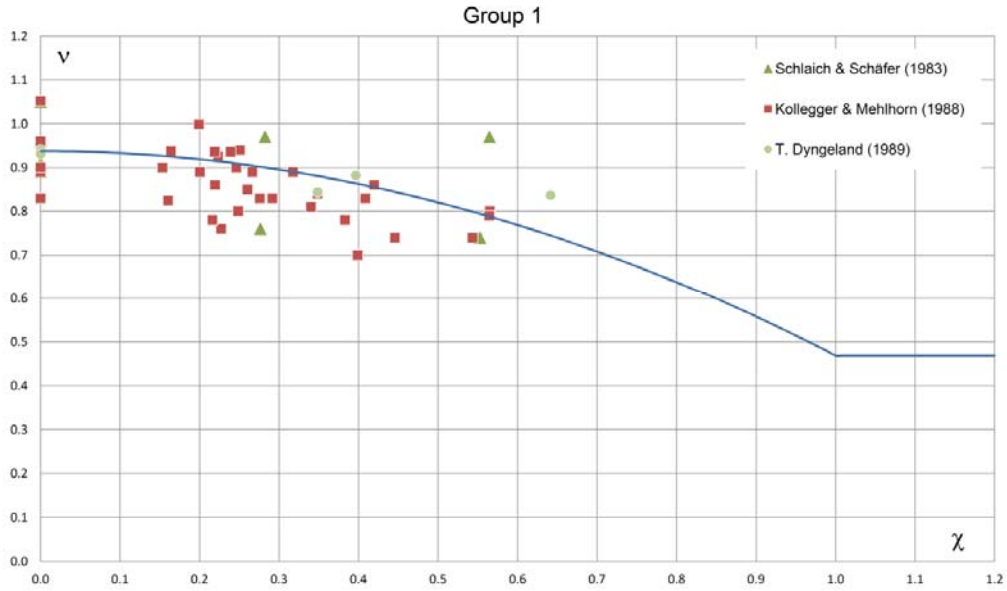

Figure 3.3 ν-formula compared with tests in Group 1 with average $f_{cs}/f_c = 0.94$.

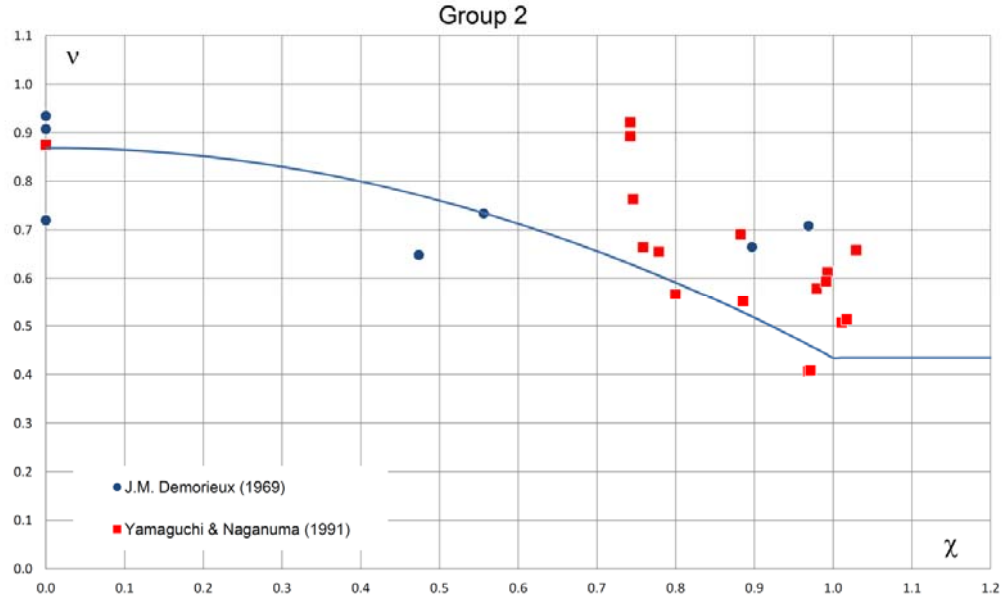

Figure 3.4 ν-formula compared with tests in Group 2 with average $f_{cs}/f_c = 0.87$.

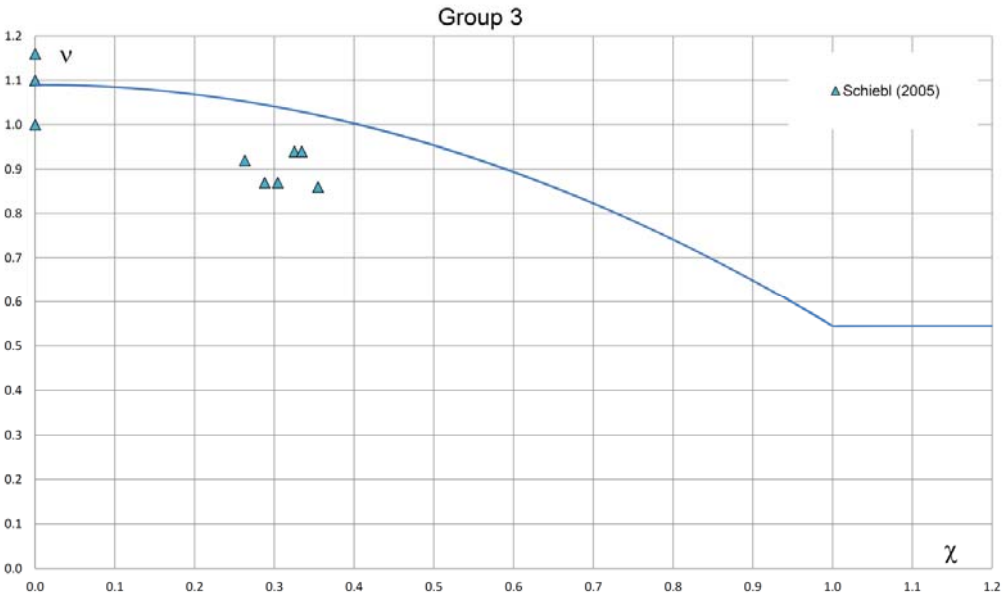

Figure 3.5 ν-formula compared with tests in Group 3 with average $f_{cs}/f_c = 1.09$.

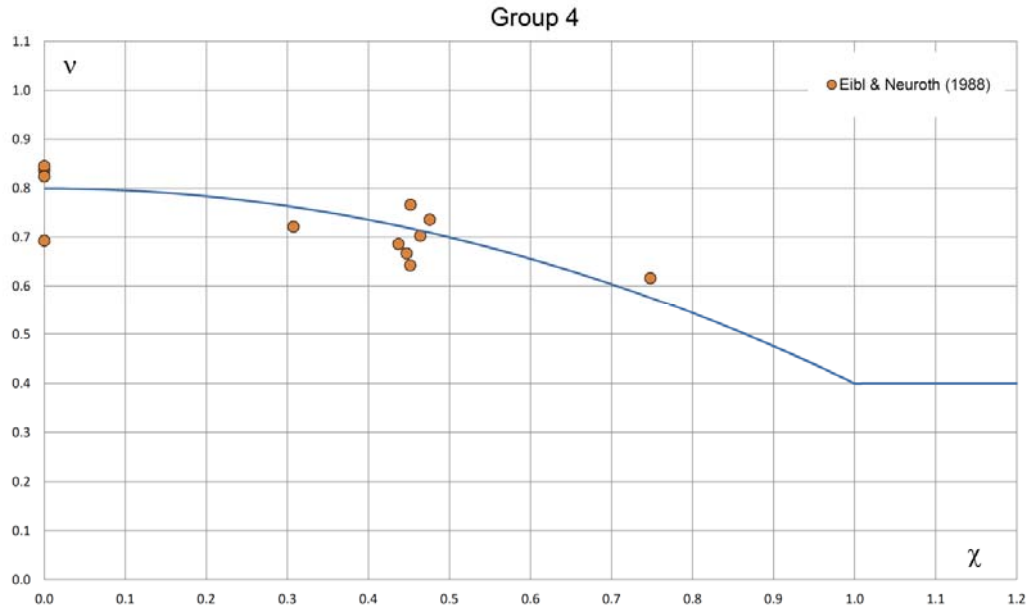

Figure 3.6 ν-formula compared with tests in Group 4 with average $f_{cs}/f_c = 0.80$.

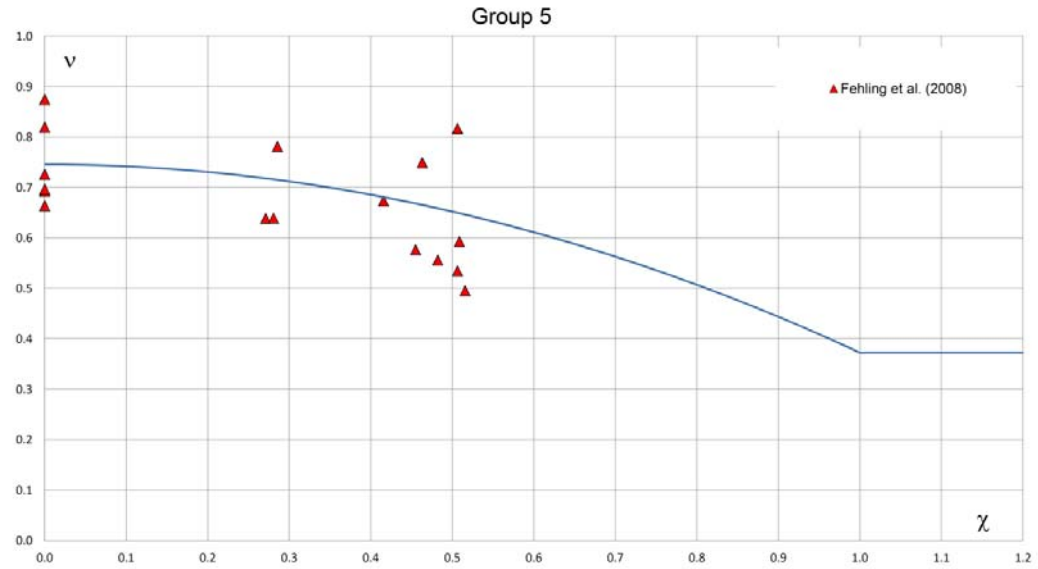

Figure 3.7 ν-formula compared with tests in Group 5 with average $f_{cs}/f_c = 0.75$.

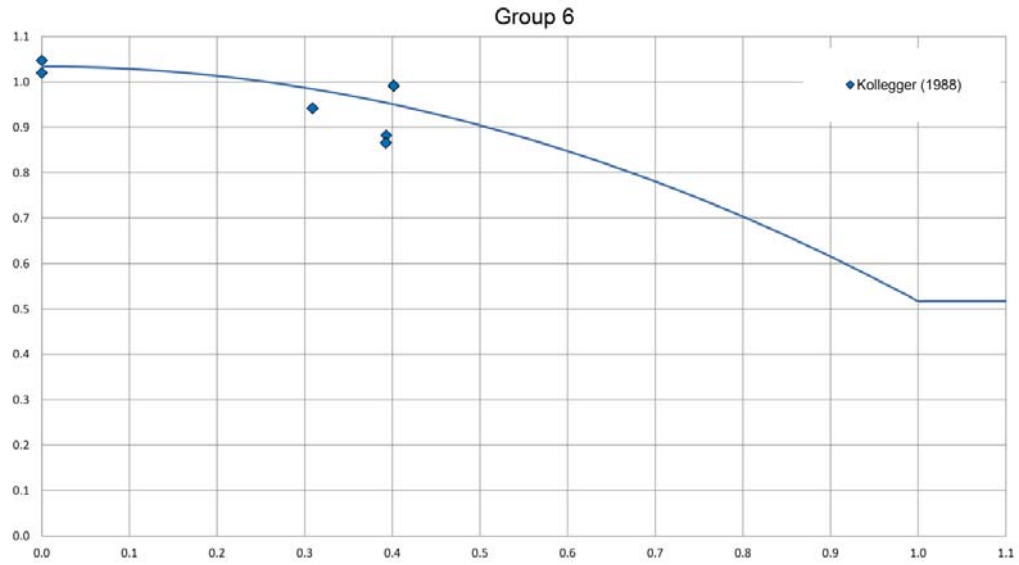

Figure 3.8 ν-formula compared with tests in Group 6 with average $f_{cs}/f_c = 1.03$.

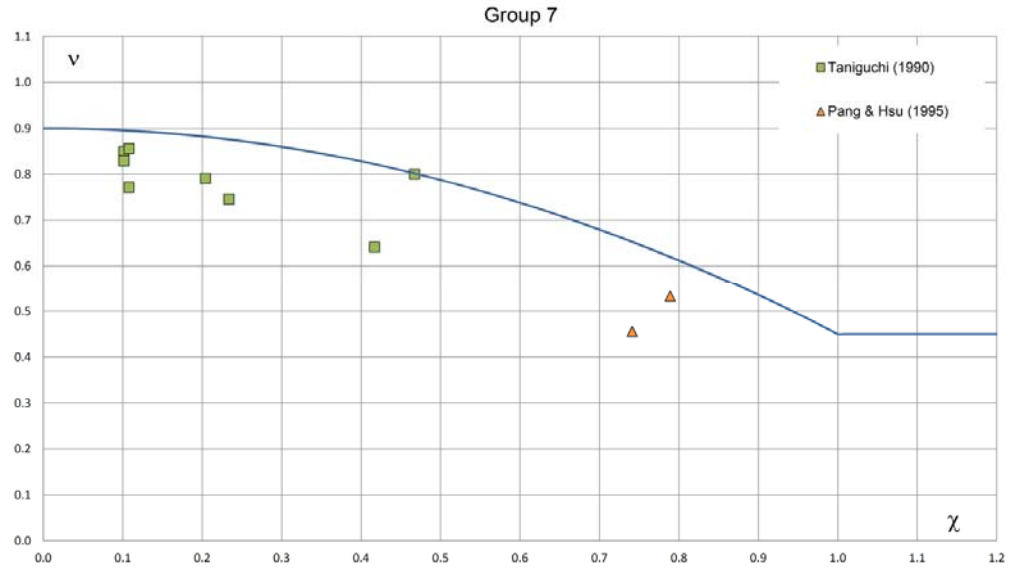

Figure 3.9 ν-formula compared with tests in Group 7 with assumed $f_{cs}/f_c = 0.90$.

4. Discussion

In the previous Chapter, we found $C = 0.244$ by calibration with tests. When adopting this value, we may rewrite formula (2.12) as follows:

$$\chi = 1.95\rho\sqrt{\frac{\sigma_s}{f_t}} \tag{4.1}$$

If we as σ_s insert the yield stress, which is usually done in design situations, and if we assume f_y = 500 MPa, f_t = 2 MPa and ρ = 1 % (typical values in practice) then we find χ = 0.31. This means, according to the physical interpretation of χ, that internal cracking will extend into about 1/3 of the crack distance a, while the remaining 2/3 of the zone stay uncracked. To render full penetration of internal cracks, i.e. χ = 1, would require ρ = 3.24 % (still with $\sigma_s = f_y$ = 500 MPa and f_t = 2 MPa). This is a very high reinforcement ratio, which is rarely seen in practice. Indeed, as seen in Chapter 3, very few tests had χ > 1. Even in such cases, the values were quite close to 1 (see the data points in Figure 3.4). These particular tests are from the series by Yamaguchi and Naganuma (1991) where the specimens had a reinforcement ratio of 4.28 %. It seems that for practical use, we will rarely have to deal with the second equation in (2.11).

In practice, we may have compression fields crossed by an orthogonal reinforcement mesh with different reinforcement ratios as well as reinforcement stresses in the two directions. Such situations can be dealt with in a conservative way by inserting the largest reinforcement stress, typically the yield stress, and the largest reinforcement ratio into Eq. (4.1).

A more serious problem arises when the compression field at the ultimate state is crossed by one or more systems of macro cracks. Such macro cracks (initial cracks) typically stem from earlier loading stages, when the concrete and the reinforcement still behave elastically. Depending on the angle between the compression field and the initial cracks, there might or might not be a danger for sliding failure in these initial, macro cracks. The ν-formula developed in this paper does not account for the situation with sliding in initial cracks. Sliding failure in an initial crack can be included by imposing - in the direction of the macro crack - a modified Coulomb failure criterion with a reduced cohesion in the order of 50% of the cohesion of the virgin concrete (i.e. concrete without macro cracks). Details on how this is done may be found in Nielsen & Hoang (2011), Section 4.6.2. A conservative approach in this regard would be to assume macro cracking in all directions. In that case, the resulting effectiveness may roughly be taken as $\nu = \nu_s\nu_o$, where $\nu_s \sim 0.5$ is the effect of sliding in initial cracks and ν_o is calculated from formula (2.11) and reflects the effect of internal cracking.

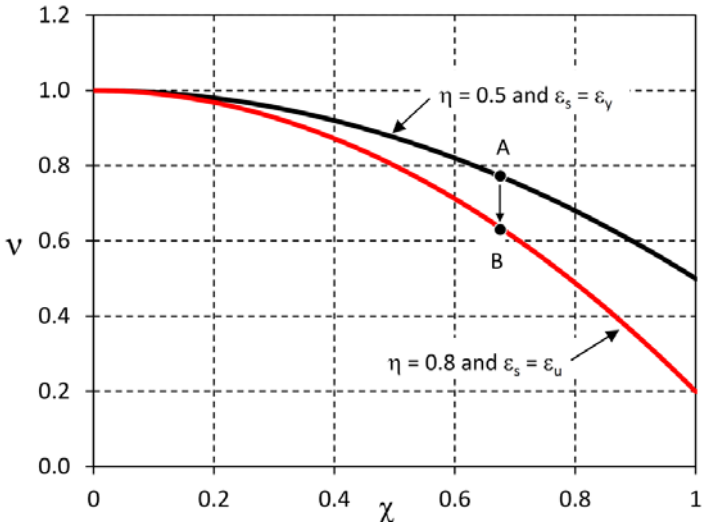

Figure 4.1 Possible concept for calculation of the additional strength reduction when the reinforcement is stressed to yielding and the strain increases from ε_y to ε_u.

In the preceding we have calibrated the ν-formula with test results, where the transverse reinforcement strain is less than or in the order of ε_y. On this basis, we have chosen $\eta = 0.5$. The interesting question now is how to deal with situations where the reinforcement is tensioned to several times the yield strain, say, 15 – 20 times ε_y?

Tests by e.g. Berlabi & Hsu (1995) have shown that further strength reduction may take place when the tensile strain increases to several times the yield strain. Such further reductions cannot be captured by the present formula. This is so because χ and thereby ν would remain unchanged once $\sigma_s = f_y$. Hence, if the formula should be further developed to deal with the situation above, we would probably have to work with a varying damage parameter η, possibly expressed as a function of the reinforcement strain since this would be a way to reflect crack widths (see also discussion in Section 2.2).

We are at present not able to formulate how the damage parameter η should increase when the transverse reinforcement strain increases. Nevertheless, we may try to study some implications of such an approach. For this purpose we assume, rather arbitrary, that $\eta = 0.8$ when the disk is subjected to the maximum possible transverse reinforcement strain, namely $\varepsilon_s = \varepsilon_u$. The strength reductions according to formula (2.11) with $\eta = 0.8$ and $\eta = 0.5$ have been plotted in Figure 4.1. Note that the graphs have deliberately been drawn only for χ up to 1 as this would be sufficient in most practical cases. For simplicity, we have used $f_{cs}/f_c = 1$. As indicated in the figure, the graph for $\eta = 0.5$ may be assumed to apply for $\varepsilon_s = \varepsilon_y$ (this strain was the upper limit when selecting the test results in Chapter 3 for model

calibration). Now, from Figure 4.1 we can for any fixed value of χ determine the *maximum additional strength reduction*, when the reinforcement strain increases from $\varepsilon_s = \varepsilon_y$ to $\varepsilon_s = \varepsilon_u$. This has been demonstrated by the drop from point A to point B in the figure.

It is interesting in this context that the ratio between ν for $\varepsilon_s = \varepsilon_y$ (i.e. point A) and ν for $\varepsilon_s = \varepsilon_u$ (i.e. point B) will increase as χ increases. For instance, with the assumptions made for the graphs, we find for $\chi = 1$ a drop from $\nu = 0.5$ to $\nu = 0.2$, i.e. 60 % additional reduction. For $\chi = 0.5$ on the other hand, the additional reduction only amounts to 9 %.

Of course, we must not delve too much into these numbers but rather focus on the fact that the additional strength reduction becomes more significant for larger values of χ. This seems very reasonable. As ε_s increases from ε_y to ε_u, we can expect the macro cracks to open wider while the internal cracks will turn into actual local punching failures with pull out of concrete cones and local debonding of reinforcing bars. This, however, will for low χ - values only lead to severe damages locally around the penetration length l, while a relatively large part of the concrete between adjacent primary cracks will remain intact. This is so because low values of χ correspond to relatively little extent of internal cracking, large distances between primary cracks and small reinforcement ratios. Large χ - values, on the other hand, mean high reinforcement ratios, shorter crack distances and internal cracks in a larger part of the zones between adjacent primary cracks. In such cases, it is easier to imagine that the internal cracks propagate to join adjacent primary cracks. This would lead to a closely spaced crack system and results in debonding and damages at a much larger scale than the case with low χ - values.

How to handle situations with large transverse strains is also a problem that arises when working with the aforementioned ν-formula proposed by Zhang (1997). In this context, an approach different from the one described above has been suggested to include the effect of large reinforcement strains. Details may be found in Nielsen & Hoang (2011), page 238 -239.

5. Conclusion

A simple semi-empirical formula for the compressive strength of reinforced concrete disks with transverse tension has been proposed. The formula is equivalent to a so-called ν-formula when used in relation to plastic design methods.

The formula contains two dimensionless parameters; the C-factor and the damage factor η. The formula has been calibrated with 127 test results from various test series. By choosing $\eta = 0.50$ and $C = 0.244$, we found the mean value of the ratio between tested strength and calculated strength to be $\nu_{test}/\nu_{cal} = 1.0$. The standard deviation was 0.145. Only tests with transverse strains less than or in the order of the reinforcement yield strain have been considered.

The formula appears as follows when inserting the calibration parameters:

$$\nu = \frac{f_{cs}}{f_c}\begin{cases} \left(1-0.5\chi^2\right) & , \ \chi \le 1 \\ 0.5 & , \chi > 1 \end{cases} \tag{5.1}$$

where χ is given by

$$\chi = 1.95\rho\sqrt{\frac{\sigma_s}{f_t}} \tag{5.2}$$

The reinforcement stress, σ_s, will in practice typically be taken as the yield stress and χ will in most cases be smaller than 1. Furthermore, to make the formula operational in practice, f_{cs}/f_c should be fixed to a constant value. In the present study we found $f_{cs}/f_c = 0.90$, the average value for all disks tested in uniaxial compression. However, in practice, we may as well adopt $f_{cs}/f_c = 1.0$ as a nominal value.

Additional strength reduction due to very large transverse strains, e.g. 15 – 20 times the reinforcement yield strain, and additional strength reduction due to sliding in initial macro cracks are not covered by formula (5.1). Brief discussions on how to handle these situations have been given in Chapter 4.

6. Symbols

a	Crack distance (for primary crack system)
A_c	Cross sectional area
$A_{surface}$	Surface area of cone
C	Dimensionless parameter
d	Diameter of reinforcement bar
f_c	Uniaxial cylinder compressive strength of concrete
f_{cs}	Uniaxial compressive strength of concrete disk
$f_{cs,red}$	Reduced strength of concrete in zones with internal cracking
f_t	Uniaxial tensile strength of concrete
f_y	Yield stress of reinforcement
$f_{0.2\%}$	Nominal yield stress (stress level corresponding to 0.2% plastic strain when released)
h	Height of cone
k	Constant
l	Penetration length of internal cracking
r	Radius of cone
t	Thickness of disk
χ	Parameter in ν-formula
ε_s	Strain in reinforcement
ε_y	Yield strain of reinforcement
ε_u	Ultimate strain of reinforcement
ε_1	Transverse strain
ε_2	Strain in direction of concrete compression
η	Damage factor
ν	Effectiveness factor
ρ, ρ_1	Reinforcement ratios
θ	Angle between compression field and reinforcement direction
σ_c	Reduced compressive strength of concrete crossed by tensioned reinforcement bars

σ_{max} Maximum applied compression stress (applied force divided by A_c)

σ_s Reinforcement tensile stress

σ_1 Applied tensile stress (i.e. $\sigma_1 = \rho\sigma_s$ or $\rho_1\sigma_s$)

τ_{max} Maximum applied shear stress

7. References

Belarbi, A. & Hsu, TH.T.C. (1995). Constitutive Laws of Softened Concrete in Biaxial Tension-Compression. ACI Structural Journal, Vol. 92 (1995), 562-573.

Demorieux, J.M. (1969). Essai de traction-compression sur modéles d'ame de poutre en beton armé. Annales de l'Institut Technique du Bâtiment et des Traveaux Publics, No. 258, Juin 1969, 980-982.

Dyngeland, T. (1989). Behaviour of reinforced concrete disks – An experimental study of reinforced concrete disks subjected to uniaxial tensile stresses and to combined tensile and compressive stresses. Institutt for Betonkonstruksjoner, Trondheim, 1989.

Eibl, J. & Neuroth, U. (1988). Untersuchungen zur Druckfestigkeit von bewehrtem Beton bei gleichzeitig wirkendem Querzug. Universität Karlsruhe, Institut für Massivbau und Baustofftechnologie, Abteilung Massivbau, 1988.

Fehling, E., Leutbecher, T., Röder, F.K. (2008). Biaxial Compression-Tension Strength of Reinforced Concrete and Reinforced Steel Fibre Concrete in Structural Disks. Structural Material and Engineering Series, No. 11, Kassel University, 2008.

Goto, Y. (1971). Cracks formed in concrete around deformed tension bars. ACI Structural Journal, Vol. 68 (1971), 244-251.

Goto, Y. & Otsuka, K. (1980). Studies on internal cracks formed in concrete around deformed tension bars. Transactions of the Japan Concrete Institute, 1980, p. 159.

Jacobsen, H.J. & Larsen, B. (2010). Compressive Strength of Reinforced Concrete Disks with Transverse Tension. B.Sc. Thesis, Department of Industrial and Civil Engineering, University of Southern Denmark, 2010.

Kollegger, J. (1988). Ein Materialmodell für die Berechnung von Stahlbetonflächentragwerken; Dissertation, Kassel University, 1988.

Kollegger J., Mehlhorn, G. (1988). Biaxale Zug-Druckversuche an Stahlbetonscheiben. AbschlussBericht zum DFG-Forschungsvorhaben Me 464/29, Forschung beriecht aus dem Fachgebiet Massivbau Nr. 6, Kassel University, 1988.

Nielsen, M.P. (2005). Beton 1 – del 3, 2. udgave (Concrete Structures 1 – part 3, 2nd edition). Department of Civil Engineering, Technical University of Denmark, Lyngby, 2005.

Nielsen, M.P. & Hoang, L.C. (2011). Limit Analysis and Concrete Plasticity. 3rd Edition, CRC Press, 2011.

Pang, X.B. & Hsu, TH.T.C. (1995). Behaviour of Reinforced Concrete Membrane Elements in Shear, ACI Structural Journal, Vol. 92, No. 6, 1995, 665-680.

Roos, W. (1994). Zur Druckfestigkeit des gerissenen Stahlbetons in scheibenförmigen Bauteilen bei gleichzeitig wirkender Querzugbeanspruchung. Dissertation, TU München, 1994.

Schieβl, A. (2005). Die Druckfestigkeit von gerissenen Scheiben aus Hochleistungsbeton und selbstverdichtendem Beton unter besonderer Berücksichtigung des Einflusses der Rissneigung. Deutscher Ausschuss für Stahlbeton, Heft 548, Beuth Verlag, Berlin, 2005.

Schlaich, J. & Schäfer, K. (1983). Zur Druck-Querzug-Festigkeit des Stahlbetons. Beton- und Stahlbetonbau 78 (1983), 73-78, Ernst &Sohn Verlag, Berlin.

Tanigushi, H., Veda, M., Higashibata, Y., Kei, T., Iwashita, K. (1990). Behaviour of RC Panels Subjected to In-Plane Loadings. In: Second International Conference on Computer Aided Analysis and Design of Concrete Structures, TU Wien, Zell am See 1990, 165-176.

Vecchio, F.J. & Collins, M.P. (1982). The response of reinforced concrete to in-plane and normal stresses. The Department of Civil Engineering, University of Toronto, Canada, Mar. 1982.

Yamaguchi, T., Naganuma, K. (1991). Experimental study on mechanical characteristics of reinforced concrete panels subjected to in-plane shear force. Journal of Struct. Constr. Engng. AIJ, No.419, Jan. 1991.

Zhang JP (1997). Strength of Cracked Concrete, Part 3 – Load Carrying Capacity of Disks Subjected to In-plane Stresses. Department of Structural Engineering and Materials, Technical University of Denmark, Series R, No. 18, 1997.

Appendix: Summary of Selected Test Results

Table A.1 Selected tests by Schlaich and Schäfer (1983).

Test specimen	Loading type	Type of reinforcement	Bar spacing	Cover to reinforcement in tension- /compression direction	Reinforcement ratio	Applied tensile stress in the reinforcement	Reduction of compressive strength	Cylinder compressive strength
No.			a	c	ρ	σ_s	σ_c/f_c	f_c
			[mm]	[mm]	[%]	[MPa]	[%]	[MPa]
$\theta = 0°/90°$								
1	b	S1	50	45/35	1.57	500	74	23.6
3	u	S1	50	45/35	1.57	0	91	23.6
5	b	S1	100	45/35	0.79	500	97	21.7
7	u	S1	100	45/35	0.79	0	105	21.7
$\theta = \pm 45°$								
2	b	S1	100	45/35	0.79	500	76	23.6
4	u	S1	100	45/35	0.79	0	89	23.6
6	b	S1	50	45/35	1.57	500	97	21.7
8	u	S1	50	45/35	1.57	0	96	21.7

Notations:

u uniaxial compression

b biaxial tension-compression (proportional loading)

S1 Reinforcement type BSt 500/550 RK, d = 10 mm

Table A.2 Selected tests by Kollegger and Mehlhorn (1988).

Test specimen	Loading type	Type of reinforcement	Bar spacing	Cover to reinforcement in tension- /compression direction	Reinforcement ratio	Applied tensile stress	Reduction of compressive strength	Cylinder compressive strength
No.			a	c	ρ	σ_1	σ_c/f_c	f_c
			[mm]	[mm]	[%]	[MPa]	[%]	[MPa]
θ = 0°/90°								
EGE102	b	S1	100/100	8.5/18.5	1.57	1.9	83	17.8
EGE103	b	S1	100/100	8.5/18.5	1.57	1.2	85	11.2
EGE104	b	S1	100/100	8.5/18.5	1.57	2.2	89	17.0
EGE105	b	S1	100/100	8.5/18.5	1.57	3.5	86	14.1
EGE110*	b	S1	100	8.5/18.5	1.57	6.3	80	13.9
EGE111	b	S1	100/100	8.5/18.5	1.57	6.6	79	15.3
EGE112	b	S1	100/100	8.5/18.5	1.57	6.7	74	17.8
EGE113	b	S1	100/100	8.5/18.5	1.57	0	89	9.5
EGE114	b	S1	100/100	8.5/18.5	1.57	1.2	94	13.0
EGE115	b	S1	100/100	8.5/18.5	1.57	2.8	78	13.0
EGE116	b	S1	100/100	8.5/18.5	1.57	4.4	74	17.5
θ = 0°/90°								
EGE601	b	S3	100/100	12/18.5	0.66	2.3	86	14.5
EGE602	b	S3	100/100	12/18.5	0.66	1.2	90	16.6
EGE603	u	S3	100/100	12/18.5	0.66	0	96	12.9
EGE701	b	S4	100/100	12/18.5	0.66	2.4	76	13.8
EGE702	b	S4	100/100	12/18.5	0.66	2.4	78	16.8
EGE703	u	S4	100/100	12/18.5	0.66	0	83	12.3

Notations:

u uniaxial compression

b biaxial tension-compression

S1 BSt 420/500 RU, d = 10 mm

S3 BSt 420/500 RU, d = 6.5 mm

S4 BSt 500/550 RU, d = 6.5 mm

*only reinforcement in θ = 0°

Table A.2 (Continued..)

Test specimen	Loading type	Type of reinforcement	Bar spacing	Cover to reinforcement	Reinforcement ratio	Applied tensile stress	Reduction of compressive strength	Cylinder compressive strength
No.			a	c	ρ	σ_1	σ_c/f_c	f_c
			[mm]	[mm]	[%]	[MPa]	[%]	[MPa]
Series 3 - θ = 0°/90°								
EGE851	b	S2	100/100	10/18.5	1.13	4.8	70	17.0
EGE852	b	S2	100/100	10/18.5	1.13	2.0	83	12.9
EGE853	b	S2	100/100	10/18.5	1.13	3.4	81	16.1
MGE851	b	M1	100/100	10/18.5	1.13	4.8	83	15.4
MGE852	b	M1	100/100	10/18.5	1.13	2.0	89	14.8
MGE853	b	M1	100/100	10/18.5	1.13	3.4	84	14.6
Series 4 - θ = ±45°								
EGE6F1	b	S3	100/100	12/18.5	0.66	2.0	89	15.8
EGE6F2	b	S3	100/100	12/18.5	0.66	2.5	93	16.0
EGE6F3	b	S3	100/100	12/18.5	0.66	2.9	90	14.6
EGE6F4	b	S3	100/100	12/18.5	0.66	3.2	80	17.1
EGE6F5	u	S3	100/100	12/18.5	0.66	0	90	18.9
EGE6F7	b	S3	100/100	12/18.5	0.66	1.4	82	18.8
EGE6F8	b	S3	100/100	12/18.5	0.66	1.8	100	13.1
EGE7F1	b	S4	100/100	12/18.5	0.66	2.4	94	15.9
EGE7F2	b	S4	100/100	12/18.5	0.66	2.8	94	15.3
EGE7F3	b	S4	100/100	12/18.5	0.66	1.4	94	17.3
EGE7F4	u	S4	100/100	12/18.5	0.66	0	105	14.2

Notations:

u uniaxial compression

b biaxial tension-compression

S2 BSt 500/500 RU, d = 8.5 mm

S3 BSt 420/500 RU, d = 6.5 mm

S4 BSt 500/550 RU, d = 6.5 mm

M1 BSt 500/550 RU, d = 8.5 mm

Table A.3 Selected tests by Kollegger (1988).

Test specimen	Loading type	Type of reinforcement	Bar spacing in both directions	Cover to tensile reinforcement	Reinforcement ratio	Applied tensile stress	Maximum applied compression	Concrete compressive strength	Cylinder compressive strength	Reduction of compressive strength
No.			a	c	ρ	σ_1	σ_{max}	σ_c	f_c	σ_c / f_c
			[mm]	[mm]	[%]	[MPa]	[MPa]	[MPa]	[MPa]	[%]
θ = 0/90°										
PK03	b	S1	90	6/12.5	1.06	5.53	23.4	19.1	19.30	99
θ = ±45°										
PK02	b	S1	90	6/12.5	1.06	3.28	15.00	18.28	19.40	94
PK04	b	S1	90	6/12.5	1.06	5.42	12.40	17.82	20.20	88
PK06	u	S1	90	6/12.5	1.06	0.00	20.30	20.30	19.90	102
PK07	b	S1	90	6/12.5	1.06	5.50	12.60	18.10	20.90	87
PK08	u	S1	90	6/12.5	1.06	0.00	19.90	19.90	19.00	105

Notation:

b biaxial tension-compression

S1 f_y = 660 MPa, d = 6.5 mm

Table A.4 Selected tests by Schieβl (2005).

Test specimen	Loading type	Type of reinforcement	Bar spacing	Cover to reinforcement	Reinforcement ratio	Applied tensile strain	Reduction of compressive strength	Cylinder compressive strength
No.			a	c	ρ	ε_1	σ_c / f_c	f_c
			[mm]	[mm]	[%]	[‰]	[%]	[MPa]
Normal Strength Concrete (NSC) - $\theta = 0^\circ$								
NB-1-0-1	u	S1	58	44	1.36	-	110	42.70
NB-1-0-2	u	S1	58	44	1.36	-	100	41.70
NB-1-90-0-1	b	S1	58	44	1.36	1.44	94	38.30
NB-1-90-0-2	b	S1	58	44	1.36	1.70	86	37.60
NB-1-90-0-3	b	S1	58	44	1.36	1.57	94	40.60
NB-1-90-1-1	b	S1	58	44	1.36	4.94	63	38.80
High Strength Concrete (HSC) - $\theta = 0^\circ$								
HLB-1-0-1	u	S1	58	44	1.36	-	116	74.10
HLB-1-0-2	u	S1	58	44	1.36	-	110	74.70
HLB-1-90-0-1	b	S1	58	44	1.36	1.65	87	81.70
HLB-1-90-0-2	b	S1	58	44	1.36	1.78	87	76.00
HLB-1-90-0-3	b	S1	58	44	1.36	1.30	92	72.80
HLB-1-90-1-1	b	S1	58	44	1.36	4.69	71	76.80
HLB-1-90-1-2	b	S1	58	44	1.36	4.75	75	76.70

Notations:

u uniaxial compression

b biaxial tension-compression

S1 d = 12 mm

Table A.5 Selected tests by Dyngeland (1989)

Test specimen	Loading type	Type of reinforcement	Bar spacing	Cover to tensile reinforcement	Reinforcement ratio	Applied Tensile stress	Maximum applied compressiion	Maximum concrete compression	Cylinder compressive strength	
No.	-		a	c	ρ	σ_1	σ_{max}	σ_c	f_c	σ_c/f_c
-	-		[mm]	[mm]	[%]	[MPa]	[MPa]	[MPa]	[MPa]	[%]
θ = 0/90°										
CS5	u	S1	90/90	10/18	1.12	0.00	25.69	20.05	21.33	94
CS6	b	S1	90/90	10/18	1.12	5.61	25.69	20.09	22.78	88
θ = ±45°										
CS7	u	S2	90/90	10/18	2.51	0.00	17.91	17.91	19.25	93
CS8	b	S1	90/90	10/18	1.12	4.20	14.01	18.21	21.57	84
CS9	b	S2	90/90	10/18	2.51	6.54	12.77	19.31	23.08	84

Notations:
u uniaxial compression
b biaxial tension-compression
S1 K500TS; f_y = 500 MPa; d = 8 mm
S2 K500TS; f_y = 500 MPa; d = 12 mm

Table A.6 Selected tests by Eibl and Neuroth (1988)

Test specimen	Loading type	Type of reinforcement	Bar spacing	Cover to tensile reinforcement	Thickness of the disk	Reinforcement ratio	Applied reinforcement stress	Cylinder compressive strength	Maximum concrete compression	Reduction of compressive strength
No.		-	a	c	t	ρ	σ_s	f_c	σ_c	σ_c / f_c
		-	[mm]	[mm]	[mm]	[%]	[MPa]	[MPa]	[MPa]	-
$\theta = 0^\circ$										
2	u	S1	130	70	160	1.5	0	26.3	22.0	0.84
3	u	S1	130	70	160	1.5	0	27.5	19.0	0.69
10	u	S1	130	70	160	1.5	0	31.4	26.5	0.85
5	b	S1	130	70	160	1.5	420	28.8	18.5	0.64
9	b	S1	130	70	160	1.5	420	28.7	22.0	0.77
6	b	S2	65	25	160	1.5	420	30.0	20.0	0.67
7	b	S2	65	25	160	1.5	420	32.8	22.5	0.69
11	u	S2	100	15	160/100	1.6	0	32.2	26.5	0.82
12	b	S2	100	15	160/100	1.6	420	33.4	23.5	0.70
13	b	S2	100	15	160/100	1.6	420	30.3	26.5	0.74
14	b	S3	100	92	200	1.0	420	29.1	21.0	0.72
0	b	S3	100	32	80	2.5	420	32.5	20.0	0.62

Notations:

u uniaxial compression

b biaxial tension-compression

S1 f_y = 420 MPa; d = 20 mm

S2 f_y = 420 MPa; d = 10 mm

S3 f_y = 420 MPa; d = 16 mm

Table A.7 Selected tests by Demorieux (1969)

Test specimen	Loading type	Type of reinforcement	Bar spacing	Cover to reinforcement	Reinforcement ratio	Applied reinforcement stress	Cylinder compressive strength	Maximum concrete compression	Reduction of compressive strength
No.		-	a	c	ρ	σ_s	f_c	σ_c	σ_c / f_c
		-	[mm]	[mm]	[%]	[MPa]	[MPa]	[MPa]	[%]
$\theta = 0^\circ$									
CY9A	b	S1	36	16	1.51	500	37.07	24.03	65
CY9B	u	S1	36	16	1.51	0	37.07	26.67	72
CY10A	b	S1	36	16	1.51	500	19.52	14.32	73
CY10B	u	S1	36	16	1.51	0	19.52	18.24	93
CY11A	b	S2	50	15	2.79	500	33.93	22.56	66
CY11B	u	S2	50	15	2.79	0	33.93	30.79	91
CY12A	b	S3	72	14	3.01	500	33.93	24.03	71
CY12B	u	S3	72	14	3.01	0	33.93	30.79	91

Notations

u uniaxial compression

b biaxial tension-compression

S1 f_y = 500 MPa; d = 6 mm

S2 f_y = 500 MPa; d = 10 mm

S3 f_y = 500 MPa; d = 12 mm

Table A.8 Selected tests by Yamaguchi and Naganuma (1991).

Data also found in Zhang (1997).

Test specimen	Loading type	Type of reinforcement	Bar spacing	Cover to reinforcement	Reinforcement ratio	Applied tensile stress	Maximum applied compression	Maximum concrete compression	Cylinder compressive strength	Reduction of compressive strength
No.	-	-	a	c	ρ	σ_1	σ_{max}	σ_c	f_c	σ_c / f_c
-	-	-	[mm]	[mm]	[%]	[MPa]	[MPa]	[MPa]	[MPa]	[%]
$\theta = \pm 45^\circ$										
N-1	u	S1	90/90	53/75	2.87	0	26.87	26.87	30.69	88
N-2	b	S1	90/90	53/75	2.87	9.22	9.90	19.12	30.69	62
N-3	b	S1	90/90	53/75	2.87	9.71	9.51	19.22	30.69	63
$\theta = 0/90^\circ$										
N-4*	b	S1	100	53	2.58	9.90	23.44	23.44	30.70	76
N-5	b	S1	100	53	2.58	9.81	38.93	28.28	30.70	94
N-6	b	S1	100	53	2.58	9.81	38.05	27.40	30.70	90

Notations:
b biaxial tension-compression
S1 f_y = 412 MPa; D22 (US size, d = 22.23 mm)
*only reinforcement in $\theta = 0^\circ$

Table A.9 Selected tests by Yamaguchi and Naganuma (1991).

Data also found in Zhang (1997)

½½Test specimen	Loading type	Type of reinforcement	Bar spacing	Cover to reinforcement	Reinforcement ratio	Ultimate shear strength	Maximum concrete compression	Cylinder compressive strength	Reduction of compressive strength
No.	-	-	a	c	ρ	τ_{max}	σ_c	f_c	σ_c / f_c
-	-	-	[mm]	[mm]	[%]	[MPa]	[MPa]	[MPa]	[%]
θ = 0/90°									
S-21	s	S1	165/157	23/51	4.30	6.57	13.14	19.02	69
S-31	s	S1	165/157	23/51	4.30	8.34	16.67	30.20	55
S-32	s	S3	165/157	23/51	3.38	8.73	17.46	30.79	57
S-41	s	S2	165/157	23/51	4.30	11.87	23.73	38.74	61
S-42	s	S2	165/157	23/51	4.30	12.75	25.50	38.74	66
S-43	s	S2	165/157	23/51	4.30	11.86	23.73	40.99	58
S-44	s	S2	165/157	23/51	4.30	12.16	24.32	40.99	59
S-61	s	S2	165/157	23/51	4.30	15.40	30.80	60.70	51
S-62	s	S2	165/157	23/51	4.30	15.59	31.18	60.70	51
S-81	s	S2	165/157	23/51	4.30	16.18	32.36	79.63	41
S-82	s	S2	165/157	23/51	4.30	16.28	32.56	79.63	41

Notations:

s pure shear

S1 f_y = 378 MPa; D29 (US soft metric size, d = 28.65 mm)

S2 f_y = 408 MPa; D29 (US soft metric size, d = 28.65 mm)

S3 f_y = 378 MPa; D25 (US soft metric size, d = 25.40 mm)

D25 US soft metric size, d = 25.40 mm

Table A.10 Selected tests by Fehling et al. (2008)

Test specimen		Loading type	Type of reinforcement	Bar spacing	Cover to reinforcement	Reinforcement ratio	Applied tensile stress	Reduction of compressive strength	Cylinder compressive strength
No.	Name			a	c	ρ	σ_1	σ_c/f_c	f_c
				[mm]	[mm]	[%]	[MPa]	[%]	[MPa]
16	015	b	S1	100/225	25/15	1.57	6.15	67.3	45.3
5	000VK1	u	S1	100/225	25/15	1.57	0	81.9	57.0
6	000VK2	u	S1	100/225	25/15	1.57	0	69.3	49.5
7	000VK3	u	S1	100/225	25/15	1.57	0	72.6	43.8
8	005VK1	b	S1	100/225	25/15	1.57	2.75	63.9	50.1
9	005VK2	b	S1	100/225	25/15	1.57	2.91	63.9	48.8
10	020VK	b	S1	100/225	25/15	1.57	7.56	57.7	47.7
11	050VK	b	S1	100/225	25/15	1.57	8.95	55.6	52.9
12	250VK	b	S1	100/225	25/15	1.57	9.43	49.6	44.8
19	000	u	S1	100/225	25/15	1.57	0	69.6	48.1
20	Q000VK	u	S2	100	25	1.57	0	66.4	45.8
3	000VK4	u	S1	100/225	25/15	1.57	0	87.5	44.7
4	005VK3	b	S1	100/225	25/15	1.57	2.81	78.1	42.5
5	020VK2	b	S1	100/225	25/15	1.57	7.38	74.9	42.3
6	025VK	b	S1	100/225	25/15	1.57	8.68	81.7	41.0
7	050VK2	b	S1	100/225	25/15	1.57	9.03	59.3	43.5
8	250VK2	b	S1	100/225	25/15	1.57	9.24	53.4	46.4

Notation:

u uniaxial compression

b biaxial tension-compression

S1 BSt 500 S; tension direction: d = 10 mm; s = 100 mm; ρ = 1.57 %.
compression direction: d = 10 mm; s = 225 mm; ρ = 0.79 %

S2 BSt 500 S; tension direction: d = 10 mm; s = 100 mm; ρ = 1.57 %

Table A.11 Selected tests by Pang and Hsu (1995)

Test specimen	Loading type	Type of reinforcement	Bar spacing	Cover to reinforcement	Reinforcement ratio	Applied tensile stress	Applied maximum compression	Maximum concrete compression	Cylinder compressive strength	Reduction of compressive strength
No.			a	c	ρ	σ_1	σ_{max}	σ_c	f_c	σ_c / f_c
			[mm]	[mm]	[%]	[MPa]	[MPa]	[MPa]	[MPa]	[%]
$\theta = \pm 45^\circ$										
A4	b	S1	189/189	30/30	2.97	11.35	11.29	22.64	42.47	53
C4	b	S1	189/189	30/30	2.97	9.20	9.95	19.15	41.99	45

Notation:

b biaxial tension-compression (of equal magnitude).

S1 f_y = 420 MPa; d = 25.2 mm

Table A.12 Selected tests by Taniguchi (1990). Data also found in Roos (1994)

Test specimen	Loading type	Type of reinforcement	Bar spacing	Cover to reinforcement	Reinforcement ratio	Applied tensile stress	Applied maximum compression	Maximum concrete compression	Cylinder compressive strength	Reduction of compressive strength
No.			a	c	ρ	σ_1	σ_{max}	σ_c	f_c	σ_c/f_c
			[mm]	[mm]	[%]	[MPa]	[MPa]	[MPa]	[MPa]	[%]
θ = ±45°										
D3A	b	S1	-	-	1.78	4.90	13.5	18.40	23.00	80
D2A	b	S1	-	-	0.89	2.45	14.7	17.15	23.00	75
D1A	b	S1	-	-	0.45	1.09	20.3	21.39	25.00	86
D1AW	b	S1	-	-	0.45	1.09	18.2	19.29	25.00	77
θ = 0/90°										
P3A	b	S1	-	-	1.39	4.90	20.4	14.75	23.00	64
P2A	b	S1	-	-	0.70	2.45	22.6	19.77	25.00	79
P1A	b	S1	-	-	0.35	1.09	22.8	21.23	25.00	85
P1AW	b	S1	-	-	0.35	1.09	22.3	20.73	25.00	85

Notation:
b biaxial tension-compression
S1 f_y = 400 MPa; d = 6 mm

Summary

It is well-known that the compressive strength of reinforced concrete disks is reduced when the compressive stress field is crossed by tensioned reinforcing bars. This paper describes a semi-empirical formula to determine the strength reduction. It is assumed that internal cracking is the main reason for the strength reduction. The extent of internal cracking depends on the bursting stresses in the transverse reinforcement. A relationship between these two important parameters has been established. On this basis, a formula for the strength reduction has been derived. The formula depends on the reinforcement stress, the reinforcement ratio, the tensile strength of concrete as well as two dimensionless parameters. These two parameters have been determined by calibration with 127 test results. When designing concrete structures by use of plasticity methods, the derived formula may be used to calculate the effectiveness factor for the general case of diagonal compression fields crossed by tensioned reinforcement.

Resumé

Det er velkendt at trykstyrken af armerede betonskiver reduceres, når trykspændingsfeltet krydses af trækpåvirkede armeringstænger. Denne artikel beskriver en semi-empirisk formel til beregning af styrkereduktionen. Det antages, at indre revnedannelse er den primære årsag til styrkereduktionen. Graden af indre revnedannelse afhænger af trækkraften i tværarmeringsstængerne. Der etableres en relation mellem indre revnedannelse og tværtrækket. På denne baggrund udledes en formel for styrkereduktionen. Formlen afhænger af armeringsspændingen, armeringsprocenten, betonens trækstyrke samt to dimensionsløse parameter. Disse to parameter findes efterfølgende ved kalibrering med 127 forsøgsresultater. I forbindelse med dimensionering efter plastiske metoder kan den udledte formel anvendes til beregning af effektivitetsfaktoren for det generelle tilfælde med et skråt betontryk som krydses af trækpåvirkede armering.

DANSK SELSKAB FOR BYGNINGSSTATIK

Anmodning om optagelse i selskabet indsendes til et af bestyrelsens medlemmer:

Mogens G. Nielsen (formand), Tlf. 45 98 60 00
Rambøll, Bredevej 2, 2830 Virum

Henrik Nielsen (sekretær), Tlf. 72 44 34 48
Vejdirektoratet, Niels Juels Gade 13, Postboks 9018, 1022 København K

Mads Nicolai Jensen (kasserer), Tlf. 88 19 10 00
Alectia, Teknikerbyen 34, 2830 Virum

Henrik Mørup, Tlf. 48 10 42 00
NIRAS, Sortemosevej 2, 3450 Allerød

Holger Koss, Tlf. 72 15 77 00
FORCE, Hjortekærvej 99, Bygning 118, 2800 Kgs. Lyngby

Jeppe Jönsson, Tlf. 45 25 17 07
BYG•DTU, Brovej. Bygning 118, 2800 Kgs. Lyngby

Lars Hauge, Tlf. 45 97 28 81
COWI, Parallelvej 2, 2800 Kgs. Lyngby.

Per Alan Olsen, Tlf. 43 48 64 17
Grontmij|Carl Bro, Granskoven 8, 2600 Glostrup

Selskabets formål er at arbejde for den videnskabelige udvikling af bygningsmekanikken - både teori for og konstruktion af alle slags bærende konstruktioner - fremme interessen for faget, virke for et kollegialt forhold mellem dets udøvere og hævde dets betydning overfor og i samarbejde med andre grene af ingeniørvidenskaben. Formålet søges bl.a. realiseret gennem møder med foredrag og diskussioner samt gennem udgivelse af "Bygningsstatiske Meddelelser".

Som medlemmer kan optages personlige medlemmer, firmaer og institutioner, som er særligt interesserede i bygningsmekanik, eller hvis virksomhed falder indenfor bygnings-mekanikkens område.

Det årlige kontingent er for personlige medlemmer 300 kr., for firmaer samt institutioner 1.800 kr. Studerende ved Danmarks Tekniske Universitet og andre danske ingeniørskoler samt indtil 2-års kandidater kan optages som juniormedlemmer uden stemmeret for et årskontingent på 80 kr. Pensionerede medlemmer med mindst 10 års medlemsanciennitet kan opnå status som pensionistmedlem med stemmeret for et årskontingent på 100 kr.

Selskabets medlemmer modtager frit "Bygningsstatiske Meddelelser", der udsendes kvartalsvis. Endvidere publiceres "Bygningsstatiske Meddelelser" på Selskabets hjemmeside www.dsby.dk. Manuskripter til optagelse i "Bygningsstatiske Meddelelser" modtages af redaktøren.